New Astronomy 56 (2017) 71–83

Contents lists available at ScienceDirect

New Astronomy

journal homepage: www.elsevier.com/locate/newast

Integrated spectral study of small angular diameter galactic open clusters

J.J. Clariá[c,a,*], A.V. Ahumada[c,a,1], E. Bica[b], D.B. Pavani[b,1], M.C. Parisi[c,a,1]

[a] Consejo Nacional de Investigaciones Científicas y Técnicas, CONICET, Godoy Cruz 2290, Ciudad Autónoma de Buenos Aires, CPC 1425FQB, Argentina
[b] Departamento de Astronomia, Universidade Federal do Rio Grande do Sul, Av. Bento Gonçalves 9500 Porto Alegre, RS-91501-970, Brazil
[c] Observatorio Astronómico, Universidad Nacional de Córdoba, Laprida 854, Córdoba, Argentina

HIGHLIGHTS

- Flux-calibrated integrated spectra for 9 galactic open clusters are presented.
- Simultaneous estimates of interstellar reddening and age are performed.
- Information independent from that derived through CM diagrams is provided.
- The results obtained show good agreement with previous photometric results.

ARTICLE INFO

Article history:
Received 9 November 2016
Revised 31 March 2017
Accepted 21 April 2017
Available online 24 April 2017

Keywords:
Galaxy: open clusters and associations: individual: Ruprecht 158
BH 92
Collinder 249
Harvard 5
Hogg 14
NGC 4463
ESO 065-C07
Pismis 23
Ruprecht 122 - Techniques: spectroscopic

ABSTRACT

This paper presents flux-calibrated integrated spectra obtained at Complejo Astronómico El Leoncito (CASLEO, Argentina) for a sample of 9 Galactic open clusters of small angular diameter. The spectra cover the optical range (3800–6800 Å), with a resolution of ∼14 Å. With one exception (Ruprecht 158), the selected clusters are projected into the fourth Galactic quadrant ($282^o < l < 345^o$) near the Galactic plane ($|b| \leq 9^o$). We performed simultaneous estimates of foreground interstellar reddening and age by comparing the continuum distribution and line strenghts of the cluster spectra with those of template cluster spectra with known parameters. We thus provide spectroscopic information independent from that derived through color-magnitude diagram studies. We found three clusters (Collinder 249, NGC 4463 and Ruprecht 122) younger than ∼40 Myr, four moderately young ones (BH 92, Harvard 5, Hogg 14 and Pismis 23) with ages within 200–400 Myr, and two intermediate-age ones (Ruprecht 158 and ESO 065-SC07) with ages within 1.0–2.2 Gyr. The derived foreground $E(B-V)$ color excesses vary from around 0.0 in Ruprecht 158 to ∼1.1 in Pismis 23. In general terms, the results obtained show good agreement with previous photometric results. In Ruprecht 158 and BH 92, however, some differences are found between the parameters here obtained and previous values in the literature. Individual spectra of some comparatively bright stars located in the fields of 5 out of the 9 clusters here studied, allowed us to evaluate their membership status. The current cluster sample complements that of 46 open clusters previously studied by our group in an effort to gather a spectral library with several clusters per age bin. The cluster spectral library that we have been building is an important tool to tie studies of resolved and unresolved stellar content.

1. Introduction

Open clusters (OCs) are among the few Galactic objects for which meaningful distances can be derived over a large range, which makes them excellent targets not only to probe the Galactic disk properties (Friel, 1995; Bonatto et al., 2006) but also to trace the disk chemical evolution (see, e.g., Bragaglia and Tosi, 2006; Chen et al., 2003, and references therein). In particular, OCs projected around the Galactic center direction play an important role as they offer the possibility of tracing the structure and evolution of the inner Galactic disk. Based on different approaches, there

* Corresponding author at: Observatorio Astronómico, Universidad Nacional de Córdoba, Laprida 854, Córdoba, Argentina. Tel.: +56 2 4633100.
E-mail addresses: claria@oac.uncor.edu (J.J. Clariá), andrea@oac.uncor.edu (A.V. Ahumada), bica@if.ufrgs.br (E. Bica), dpavani@if.ufrgs.br (D.B. Pavani), celeste@oac.uncor.edu (M.C. Parisi).
[1] Visiting Astronomer, Complejo Astronómico El Leoncito, CASLEO, operated under agreement between the Consejo Nacional de Investigaciones Científicas y Técnicas de la República Argentina and the National Universities of La Plata, Córdoba and San Juan.

http://dx.doi.org/10.1016/j.newast.2017.04.011
1384-1076/

Table 1
Cluster sample

Cluster	l (^{o})	b (^{o})	α_{2000} (h:m:s)	δ_{2000} (^{o}:':")	D (')	Trumpler class
Ruprecht 158	259.56	4.44	8:52:27	−37:34:00	2.0	III2p
BH 92	282.98	0.44	10:19:07	−56:25:00	2.0	II2p
Collinder 249*	294.85	−1.65	11:38:20	−63:22:22	65.0	III-3m,n
Harvard 5	299.97	1.97	12:27:10	−60:46:00	5.0	II3p
Hogg 14	300.08	2.94	12:28:39	−59:48:36	3.0	II3p
NGC 4463	300.64	−2.01	12:29:56	−64:47:24	6.0	I3m
ESO 065-SC07	305.99	−8.62	13:29:17	−71:16:06	4.0	III2
Pismis 23	334.67	0.43	16:23:48	−48:55:00	1.0	III2m
Ruprecht 122	344.28	1.57	16:55:08	−40:56:35	3.0	–

* Only the central part (∼2') of Cr 249 was observed

exist estimates of a total of about 25 × 10^3 or more OCs in our Galaxy (see, e.g., Piskunov et al., 2006; Bonatto et al., 2006; Portegies Zwart et al., 2010). However, in the catalogue by Kharchenko et al. (2013) only ∼2800 Galactic OCs have a resonable estimate of their fundamental parameters such as reddening, distance and age. This figure probably represents a lower limit to the possible number of OCs belonging to our Galaxy, if we take into account the recently discovered clusters and cluster candidates (see, e.g., Bica et al., 2003; Dutra et al., 2003; Borissova et al., 2011; 2014; Ramírez Alegría et al., 2014; 2016; Chené et al., 2013; Barbá et al., 2015) and the still unseen OCs deeply embedded in obscured regions as well as those which are just too faint to be detected. OC fundamental parameters have been mostly derived from color-magnitude diagrams (e.g., Dias et al., 2002; Hasegawa et al., 2008; Monteiro et al., 2017) and/or from photometric and kinematic studies of individual giants (e.g., Clariá et al., 2006; 2008). Sometimes, however, integrated spectroscopy becomes a powerful technique to study star clusters not only in our Galaxy (e.g., Santos and Bica, 1993; Schiavon et al., 2005) but also in the Large Magellanic Cloud (e.g., Santos et al., 2006; Minniti et al., 2014), in the Small Magellanic Cloud (e.g., Talavera et al., 2010; Dias et al., 2010) and even in distant galaxies (e.g., Jablonka et al., 1998; Trancho et al., 2007). In particular, in small angular size Galactic OCs, integrated spectra can provide independent information about their reddenings, ages and, in some cases, also about their metallicities (e.g., Ahumada et al., 2000).

As part of a program of systematic observations of small angular diameter Galactic OCs, we determine here foreground reddening and age for a sample of 9 OCs, 8 of which are projected onto the fourth Galactic quadrant (Table 1). Some of these clusters are embedded in dense stellar fields. They were selected considering not only their compact nature and surface brightness but also the fact that most of them have been only poorly studied. We have already reported results based on integrated spectra for 46 small angular size OCs, most of which are located in the fourth Galactic quadrant (Ahumada et al., 2000; 2001; 2007a; Palma et al., 2008). Twenty six out of these 46 clusters had not been previously studied so that their reddenings and ages were derived for the first time from their integrated spectra.

Besides determining cluster parameters with integrated spectra, we tie this individual cluster information to the resolved/integrated issue of stellar populations: (i) we study individually our previous spectral base of 46 OCs and add to it 9 other OCs; (ii) the spectroscopic technique provides essentially independent comparisons of cluster parameters to those derived by the imaging technique, such as the color-magnitude diagrams, color-color diagrams and photometric catalogues; (iii) spectroscopy is sometimes time consuming, but it is necessary to develop and validate stellar population connections. Bica (1988) first employed star cluster spectra to describe stellar populations in galaxies. That principle is now widely used in the Starlight code to the spectroscopic study of thousands of galaxies in different surveys (see, e.g., Cid Fernandes et al., 2001; López Fernández et al., 2016); (iv) our group has also been developing similar spectroscopic libraries for star clusters in the SMC and LMC (Ahumada et al., 2011, and references therein); (v) the spectral evolution by means of star cluster spectra (e.g. Santos et al., 2006) also constitutes a stepping stone to the spectroscopy understanding of galaxies;(vi) star cluster spectra have been observed to the distance of Virgo (e.g. Pierce et al., 2006), and the new generation telescopes GMT, ELT and TNT will go deeper, and consequently the present collected Milky Way and Local Group star clusters are fundamental bases for such future studies.

This paper is organized as follows. In Section 2, we present the cluster sample and the spectroscopic observations. The measurements of equivalent widths for Balmer absorption lines, as well as the methods employed to determine reddening and age values, are described in Section 3. Individual objects are described and discussed in Section 4. Concluding remarks are summarized in Section 5.

2. Cluster sample and spectroscopic data

Over 20 years, one of us (E.B.) systematically examined the Digitized Sky Survey (DSS) images for about 2000 OCs in the WEBDA/DAML02 catalogues, aiming at establishing a sample of high surface brightness OCs with relatively small angular sizes, among other purposes. That unique and important sample amounts to ≈ 100 OCs, of which 46 are part of our previous library, and 9 are here provided. As a rule, OCs are low surface brightness objects with large angular sizes, which makes them unsuitable for integrated spectroscopy. We conclude that our high surface brightness OC sample fraction of ≈ 5% (if we consider ≈ 2000 OCs from WEBDA and DAML02 catalogues) is very special, and CASLEO has provided us with a unique opportunity to collect those clusters' spectra.

In the current study, we have selected 8 comparatively small angular size, poorly studied OCs located near the Galacic plane ($|b| \leq 9^o$), with Galactic longitudes ranging between 260^o and 345^o. We also selected an extended OC (Collinder 249) in order to observe only its central part of about 2' in the sky. Fig. 1 shows DSS images for the cluster sample. Rectangles in this figure represent the observed regions. Table 1 lists: (1) main cluster designation, (2–5) Galactic and equatorial coordinates, and (6–7) angular size and Trumpler (1930) class taken from Archinal and Hynes (2003). The clusters are ordered according to their increasing Galactic longitudes.

The spectroscopic observations analyzed in this study were carried out at Complejo Astronómico El Leoncito (CASLEO) in San Juan (Argentina), using the "Jorge Sahade" 2.15 m Ritchey-Chrétien telescope during one night in May 2003, four nights in March 2004 and two nights in March 2005. We employed a CCD camera attached to the REOSC spectrograph in the simple mode. The detector was a Tektronics chip of 1024 × 1024 pixels of size 24 μm × 24 μm; one pixel corresponds to 0.94" on the sky. The adopted observational strategy was exactly the same as in previous observing runs, namely, the slit was set in the East–West direction and the observations were carried out by scanning the slit across the objects in the North–South direction. In some cases, however, the slit was appropriately rotated to include most of the cluster body. In the most compact clusters, each star within our area of interest (rectangles in Fig. 1) crossed the slit a larger number of times than in the largest objects. By "area of interest" we mean either the cluster nucleus or else the region of denser stellar concentration. In some cases, when one or more bright stars dominate the integrated light, individual spectra of all or some of these bright stars were observed (see Section 4). The Galactic extinction curve (Cardelli et al., 1989) is featureless in our domain, while the cluster

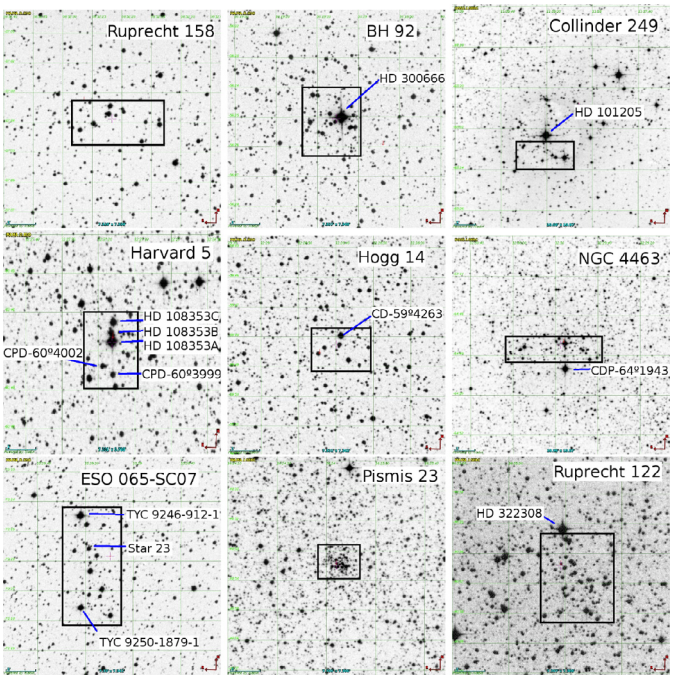

Fig. 1. DSS images for the cluster sample. Rectangles represent the scanned regions in the observations. North is up and East is to the left.

Table 2
Observation log of selected clusters

Cluster	Date	Exposure (s)	Total S/N (5200-5500 Å)
Ruprecht 158	March 23, 2004	2 × 900; 3 × 1000	45
BH 92	March 22, 2004	9 × 600	49
Collinder 249	March 24, 2004	6 × 600; 1 × 200; 1 × 120	20
Harvard 5	March 23, 2004	6 × 600	30
Hogg 14	March 12, 2005	2 × 900; 2 × 400	30
NGC 4463	March 17, 2005	2 × 900; 2 × 480; 2 × 120	41
ESO 065-SC07	March 21, 2004	6 × 600; 3 × 700	20
Pismis 23	March 22, 2004	1 × 900; 1 × 1800	20
	May 27, 2003	2 × 1800	
Ruprecht 122	March 17, 2005	2 × 480; 2 × 1200	26

spectra present Balmer lines and/or metal lines and atomic bands. We used a grating of 300 grooves/mm, which produces an average dispersion in the observed region of ≈ 140 Å/mm (3.46 Å/pixel). The useful spectral coverage was typically ≈ 3800–6800 Å. The slit width was 400 μ (≈ 4.2" on the sky), providing a resolution of 14 Å as measured from the full width at half-maximum (FWHM) in the Cu-Ar-Ne lines of the comparison lamps. On the other hand, the slit length projected onto the chip (4.7') provided a wide range of pixel rows for background subtractions. The standard stars LTT 3864, LTT 6248 and EG 274 from the list of Stone and Baldwin (1983) were observed every night for flux calibrations. Bias, darks, dome and twilight sky and Cu-Ar-Ne lamp flats were taken for reduction purposes.

In order to gather cluster spectra with an acceptable signal-to-noise (S/N) ratio, we obtained a series of cluster integrated spectra with exposure times of 2–30 min for each of the sample objects so that the total exposure time varied between 0.7 and 1.8 hours, depending on each cluster's surface brightness. The journal of observations is provided in Table 2, whose columns give in succession: (1) cluster designation, (2) date of observation, (3) number of exposures and duration in seconds and (4) the resulting S/N ratio of the spectra measured in the (5200–5500 Å) spectral interval.

Reductions were carried out with the Image Reduction and Analysis Facility (IRAF[2]) software package, following standard procedures at the Observatorio Astronómico de la Universidad Nacional de Córdoba (Argentina). Background sky subtractions were performed using pixel rows from the same frame after removing cosmic rays from the background sky regions, taking care that no significant background residuals were present on the resulting spectra. The cluster spectra were extracted along the slit according to the cluster size and available flux. For larger objects, we scanned the slit along the north-south direction in order to better sample the cluster stellar population. Some clusters actually present angular diameters slightly larger than the total field along the slit. The spectra were obtained in these cases by scanning first one portion of the main body of the cluster from which the background sky was subtracted. We then obtained the spectrum of the remaining portion of the cluster from which we also subtracted the background sky. The final spectrum results from the sum of the two mentioned spectra. Spectra were wavelength-calibrated by fitting observed Cu-Ar-Ne comparison lamp spectra with template spectra. The rms errors involved in these calibrations are typically 0.50 Å (0.14 pixel). Atmospheric extinction corrections according to the CASLEO coefficients given by Minniti et al. (1989) were applied followed by the corresponding flux calibrations. We used standard stars for the flux calibrations that we observed each night and treated them in a standard way with IRAF reductions. The long wavelength range we used in the observations of star clusters and galaxies has been systematically explored in publications of our group for almost 30 years. We refer the reader to Ahumada et al. (2007a) and Minniti et al. (2014) papers for more details about the observations and data reduction. Besides sampling the high surface brightness parts of OCs for contrast purposes, one major concern is to subtract the airglow emission lines, mainly N2, N2+, O2, NO and OH. We adopted a compromise of the stellar and background substraction, thus obtaining a high surface brightness contrast between the cluster region and its outskirts. Note that composite magnitude and colors of star clusters show that stars fainter than the medium main-sequence range do not essentially contribute to the cluster integrated light (e.g. Santos et al., 1990).

Fig. 2 shows the resulting flux-calibrated integrated spectra of the observed OCs. Spectra are in relative flux (F_λ) units, normalized at $\lambda \approx 5800$ Å, and shifted by different constants (except fot the bottom one) to allow for comparison. Although some amount of field star contamination may be expected in the observed cluster integrated spectra, only bright field stars could affect these spectra significantly. This is the case in BH 92, Harvard 5, Hogg 14, ESO 065-SC07 and Ruprecht 122 (see Section 4), wherein individual spectra of some field stars were obtained and different extractions were considered in the analysis and discussion of these clusters (see Section 4).

3. Equivalent width measurements and cluster fundamental properties

Equivalent widths (EWs) in the observed cluster integrated spectra are practically unaffected by reddening so that they reflect the intrinsic stellar atmospheres cluster properties. In order to measure EWs of the Balmer lines in the cluster sample, we have taken into account both the spectral windows and flux points as defined by Bica and Alloin (1986a); 1986b); 1987). The results of the measurements for the four primary H Balmer lines are shown in Table 3, where the EWs are given in Ångström units. Typical

[2] IRAF is distributed by the National Optical Astronomy Observatories, which is operated by the Association of Universities for Research in Astronomy, Inc., under contract with the National Science Foundation

Table 3
Measurements of the equivalent widths of the four primary H Balmer lines

Cluster	Hα (6540–6586)Å	Hβ (4846–4884)Å	Hγ (4318–4364)Å	Hδ (4082–4124)Å
Ruprecht 158	5.3	5.1	6.3	5.0
BH 92	6.0	6.7	8.5	8.1
Collinder 249	Emission	0.4	5.0	4.9
Harvard 5	5.0	7.3	7.5	10.0
Hogg 14	8.1	12.1	14.4	14.3
NGC 4463	3.6	5.0	4.6	5.4
ESO 065-SC07	3.6	5.0	5.4	7.0
Pismis 23	Emission	9.0	9.8	9.8
Ruprecht 122	3.1	5.7	7.4	8.3

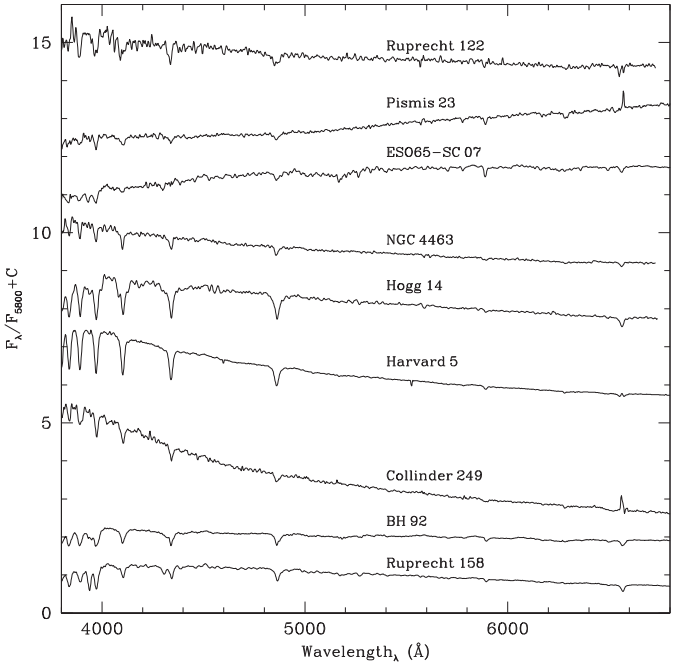

Fig. 2. Observed integrated spectra of the sample clusters. Spectra are in relative flux (F_λ) units, normalized at 5800 Å. Constants have been added to the spectra, except for the bottom one.

errors of ~10% on individual EW measurements result from tracing slightly different continua.

Bica and Alloin (1986a) showed that integrated spectra of small angular size star clusters allow us to determine their basic properties, such as reddening, age, and, in some cases, also the metallicity (e.g., Ahumada et al., 2000). A direct reddening-independent age estimate was first obtained from the EWs of the four primary H Balmer absorption lines in each cluster spectrum by interpolating these values in the age calibration of Bica and Alloin (1986b). These authors found that metallicity effects are negligible for the spectral windows that include the four Balmer lines. Age and foreground reddening $E(B-V)$ values of the selected OCs were then simultaneously derived by applying the template matching method. This was done by achieving the best possible match between the continuum and lines of the analyzed cluster integrated spectrum and these same features of a template integrated spectrum with known properties. In this process we selected, from the available template spectra, those which minimize the flux residuals calculated as the normalized difference (cluster - template) / cluster. Based on the first age estimate, we selected among the solar-metallicity cluster templates of Piatti et al. (2002, hereafter P02) and Ahumada et al. (2007a) spectral libraries, a subset of templates to compare with the observed spectrum. The final age determination was achieved

Table 4
Reddening and age determinations

Cluster	$E(B-V)$	t_{Balmer} (Myr)	$t_{Template}$ (Myr)
Ruprecth 158	−0.05	500–5000	1000
BH 92	0.35	50-500	200–350
	0.20		500
Collinder 249	0.55	< 20	2–4
Harvard 5	0.19	≤ 100	200–350
Hogg 14	0.22	100–500	200–350
NGC 4463	0.42	10–50	5–10
	0.45		30
ESO 065-SC07	0.43	1000–5000	1000
	0.25		3000–4000
Pismis 23	1.05	100–500	200–350
Ruprecht 122	0.45	10–50	40

by varying reddening and template until the best match was obtained between the chosen template and the continuum, Balmer and metal lines of the analized cluster spectrum. Basically there are no degeneracy between reddening and age. To apply the template matching method, we used the software called FISA (Fast Integrated Spectra Analyzer). This software allows fast and reasonably accurate reddening and age determinations for star clusters using their integrated spectra (Benítez-Llambay et al., 2012). To perform reddening corrections, we adopted the normal reddening law of Seaton (1979) and the most frequently used factor 3.0 for the ratio $R = A_v/E(B-V)$ between the total visual absorption and the E(B-V) color excess (Straižys, 1992). The derived reddening values are listed in Table 4, together with the age range indicated for the Balmer lines, and the age range of the templates with which the best match was obtained. The adopted $E(B-V)$ color excesses and ages are given in Table 5, together with the values reported in the literature and their corresponding references. The adopted errors for both $E(B-V)$ and age (Table 5) are only simple estimations based on the fits of the integrated cluster spectra with templates of different ages. We point out that the Balmer lines entail the cluster spectrum and template. Small mismatches may occur, especially for metal lines and molecular bands. This may also occur because of the discrete and finite number of templates. Hence the importance of new OC spectra being introduced in template libraries, for better spectral resolution and signal-to-noise ratio.

4. Discussion of individual clusters

We reported in Ahumada et al. (2007b) some preliminary findings derived from integrated spectroscopy for 6 out of the 9 clusters here analized. These results may be considered only a first approach to the estimation of $E(B-V)$ and age values. Previous reddening and age determinations by different authors for the present cluster sample are listed in Table 5. Using a combination of uniform kinematic and near-infrared (NIR) photometric data gathered in the all-sky catalogue PPMXL (Roeser et al., 2010) and in the

Table 5
Cluster parameters derived in this work and reported in the literature

Cluster	This work		Literature		
	$E(B-V)$ (mag)	Age (x10^6 yr)	$E(B-V)$ (mag)	Age (x10^6 yr)	Ref*.
Ruprecht 158	0.00± 0.05	1000± 500	0.40	1400	(1)
			0.19	1800	(8)
BH 92	0.28± 0.05	400± 200	0.19	812	(1)
			0.54	56	(8)
Collinder 249	0.55± 0.10	3± 1	0.50	4.4	(1)
			0.28–0.45	3.0	(5)
Harvard 5	0.19± 0.05	200± 100	0.21	224	(1)
			0.19	–	(3)
			0.17	–	(4)
Hogg 14	0.22± 0.05	250± 100	0.23	126	(1)
			0.28	–	(4)
NGC 4463	0.43± 0.03	19± 10	0.35	93	(1)
			0.44	–	(4)
			0.42	28	(8)
			0.39	(12-32)	(9)
ESO 065-SC07	0.34± 0.05	2200± 1000	0.29	2500	(1)
			0.48	1230	(8)
Pismis 23	1.05± 0.50	360± 150	1.46	367	(1)
			2.00	300	(6)
			1.73	700	(7)
			1.54	251	(8)
Ruprecht 122	0.40± 0.05	40± 20	0.42	40	(1)
			0.87	112	(8)

*References: (1) K13; (2) Costa et al. (2015); (3) Clariá et al. (1989); (4) MV73; (5) Baume et al. (2014); (6) Piatti and Clariá (2002); (7) Ortolani et al. (2002); (8) B11; (9) Delgado et al. (2011).

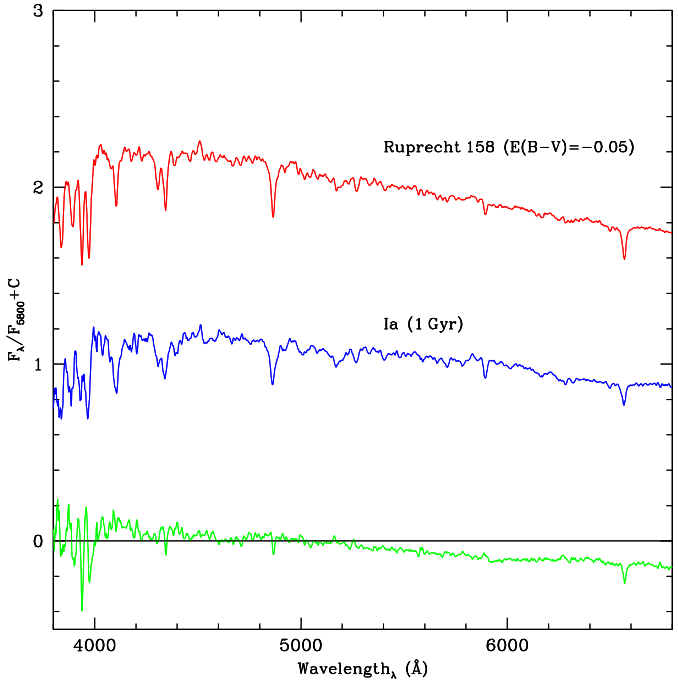

Fig. 3. Comparison between the reddening-corrected integrated spectrum of Ruprecht 158 (*top*) and the Ia template spectrum of 1 Gyr (*middle*). The corresponding flux residual according to ($F_{cluster}$ - $F_{template}$) / $F_{cluster}$ is shown at the bottom. Units as in Fig. 2.

Two-Micron All-Sky Survey (2MASS) catalogue (Skrutskie et al., 2006), Kharchenko et al. (2013, hereafter K13) reported exact positions, apparent radii, proper motions, reddennings, distances and ages for more than 2800 mostly confirmed OCs. For comparison purposes, only the ages and $E(B-V)$ color excesses derived by K13 for the present cluster sample are listed in Table 5. As shown in this table, six of the here studied OCs (Ruprecht 158, BH 92, NGC 4463, ESO 065-SC07, Pismis 23 and Ruprecht 122) were also examined by Bukowiecki et al. (2011, hereafter B11), using 2MASS data. We find, in general terms, a reasonable good agreement with K13 for 7 clusters of the present sample. A brief description of the studied OCs, as well as the results we obtained from their integrated spectra, are discussed below.

4.1. Ruprecht 158

This is a small cluster in Vela (IAU C0850-373), also designated as MWSC 1592 by Kharchenko et al. (2012, hereafter K12). Archinal and Hynes (2003, hereafter AH03) refer to this object as belonging to Trumpler (1930) class III-2p, i.e., a poor, detached cluster with no central concentration and medium range in the brightness distribution of the stars (Fig. 1). Although it could probably not be a real cluster but a fluctuation of the field star density (Vázquez et al., 2010), B11, K13 and Costa et al. (2015) derived for Ruprecht 158 an age between 1.4 and 1.8 Gyr and somewhat different $E(B-V)$ reddening values (see Table 5). Assuming that Ruprecht 158 is a real OC, its integrated spectrum shows some typical features of intermediate-age clusters (Fig. 2). In fact, not only the G-band but also the depth of the CaII K line are compatible with those of an intermediate-age object. Although rather poor, we achieved the best comparison with the Ia template (1 Gyr) from P02's spectral library of solar-metallicity open-cluster templates, correcting the observed spectrum for a small negative amount of reddening $E(B-V) = -0.05$ (Fig. 3). Since Balmer lines suggest an age close to that of the above template (Table 4), we adopted the latter as the probable best solution (Table 5). Thus, contrarily to what has been reported in previous studies (e.g., K13 or B11), Ruprecht 158 would seem to be a practically unreddened intermediate-age OC (see Table 5). Radial velocity measurements of a few stars in the cluster field could help to confirm or deny the physical reality of this cluster.

4.2. BH 92

First recognized as an OC by van den Bergh and Hagen (1975), this small size object (IAU C1017-561), also known as MWSC 1791 (K12), seems to be a detached, relatively poor and faint OC in the Vela constellation. It shows the typical morphology of a Trumpler class II-2p, which is characterized by a little central concentration of member stars and a medium-range of bright stars (Fig. 1). BH 92 presents the dominant bright red giant star HD 300666 close of its center (Fig. 1). The EWs of the Balmer lines in the observed integrated spectrum (Fig. 2) indicate an age younger than 1 Gyr (Table 4). This spectrum resembles the Yg template (200–350 Myr) of P02's library, once corrected for $E(B-V) = 0.20$ (Fig. 4). The continuum distribution, the Balmer jump and also the presence and depth of spectral lines are very similar in both spectra. Nevertheless, as shown in the same figure, a reasonable match is also found when the cluster spectrum, corrected for $E(B-V) = 0.35$, is compared to the P02's Yh template of 500 Myr. We adopted intermediate reddening and age values for BH 92 (Table 5). Therefore, this cluster seems to be slightly younger than was reported by K13 but clearly older than was estimated by B11 (Table 5). According to Nesterov et al. (1995), the dominant star HD 300666 is a M0-type object. In Fig. 5 we show that the reddening-corrected individual spectrum of HD 300666 compares reasonably well with the M0 III template from Silva and Cornell (1992, hereafter SC92). Inspecting the position of this star in the color-magnitude diagrams (CMDs) of K13, we conclude that this is very probably a luminous red giant cluster member so its contribution was taken into account in the cluster integrated spectrum. It is worth mentioning that, although there are new empirical stellar libraries (see, e.g., Chen et al., 2014,

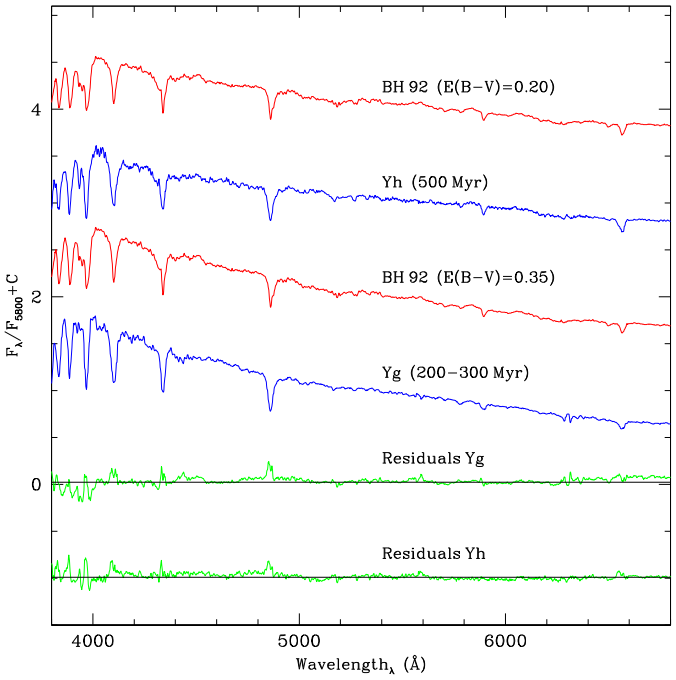

Fig. 4. *From top to bottom*: integrated spectrum of BH 92 corrected for $E(B-V)$ = 0.20, Yh template spectrum of 500 Myr, cluster spectrum corrected for $E(B-V)$ = 0.35, Yg template spectrum of (200–300 Myr), and corresponding flux residuals between both comparisons. Units as in Fig. 2.

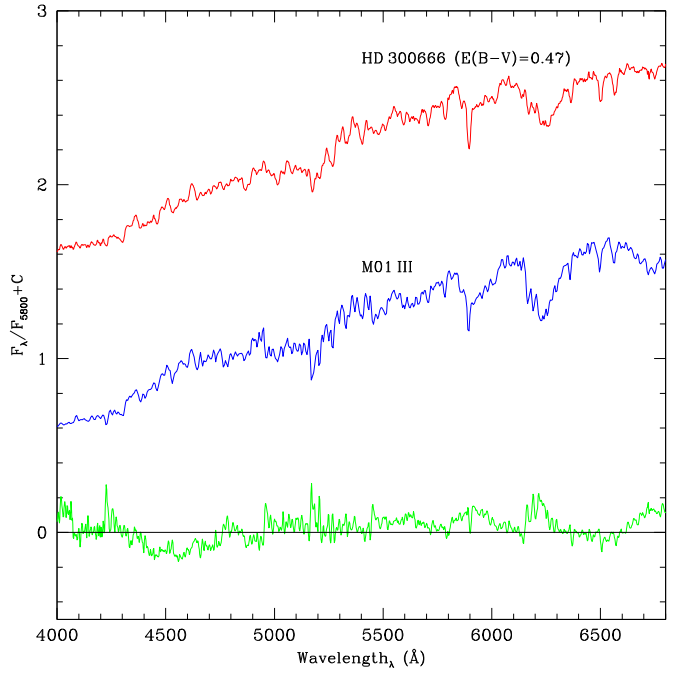

Fig. 5. Individual spectrum of the dominant star of BH 92 (HD 300666) corrected for $E(B-V)$ = 0.47 (*top*), the SC92 template spectrum which best matches it (*middle*) and the flux residual according to (F_{star} - $F_{template}$) / F_{star} (*bottom*). Units as in Fig. 2.

and references therein), the one of SC92 is probably the most complete and the easiest to use, according to our purposes.

4.3. Collinder 249

This extended object (IAU C1134-627), also referred to as BH 121 (van den Bergh & Hagen 1975), MWSC 1960 (K12) or "λ Cen cluster" (AH03), is centered on the star HD 101205 (V = 6.45, Fig. 1). Collinder 249 belongs to Trumpler class III3m,n and is inmmersed in the IC 2944 nebula. According to Alter et al. (1970), the entire group of brightest stars in this region is also referred to as Cen OB2 association. We took an integrated spectrum only for the central part of Collinder 249 (∼2' on the sky), excluding the bright star HD 101205. We simultaneously determined the reddening and age for Cr 249 using the Ya1 template (2–4 Myr) of P02's library, the best template match yielding $E(B-V) = 0.55$ (Fig. 6). Recently, Baume et al. (2014) studied this extended region in Scorpius and identified two young stellar groups (age ∼3 Myr) located at about 2.3 and 3.2 kpc from the Sun, respectively, characterized by a significant variable interstellar extinction ($0.28 < E(B-V) < 0.45$). The parameters here derived for the central part of Collinder 249 are compatible with these findings.

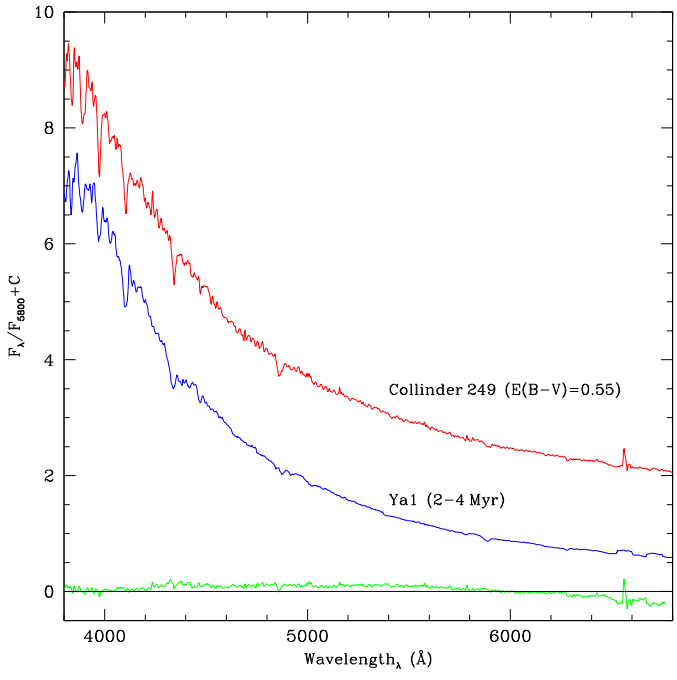

Fig. 6. Comparison between the reddening-corrected integrated spectrum of the central part of Collinder 249 (*top*) and the Ya1 template spectrum of (2–4 Myr) (*middle*). The correspoding flux residual according to ($F_{cluster}$ - $F_{template}$) / $F_{cluster}$ is shown at the bottom. Units as in Fig. 2.

4.4. Harvard 5

Situated in a region of high stellar density in the Crux constellation, Harvard 5 (Shapley, 1930), also known as Cr 258 (Collinder, 1931), BH 133 (van den Bergh and Hagen, 1975) or MWSC 2033 (K12), is a small size open cluster classified as Trumpler class II3p by AH03. Its central part appears to be dominated by the presence of the comparatively bright stars HD 108353A, HD 108353B and HD 108353C (Fig. 1). Moffat and Vogt (1973, hereafter MV73) measured photoelectrically in the UBV system 25 stars located within a radius of ≈ 5' centered at HD 108353A (Fig. 1). These stars clearly define the sequence of a young OC reddened by about $E(B-V)$ = 0.17. According to the position of HD 108353A in the CMDs of MV73, this star (MV73 No. 14) border on being a supergiant of luminosity class II. On the other hand, the individual spectrum of HD 108353C (MV73 No. 12), corrected for $E(B-V) = 0.15$, shows a noticeable resemblance to the B9 III template from SC92 (Fig. 7), so this star seems to be a late B-type giant member of Harvard 5.

The cluster integrated spectrum, without the dominant contribution of the comparatively bright blue star HD 108353A and

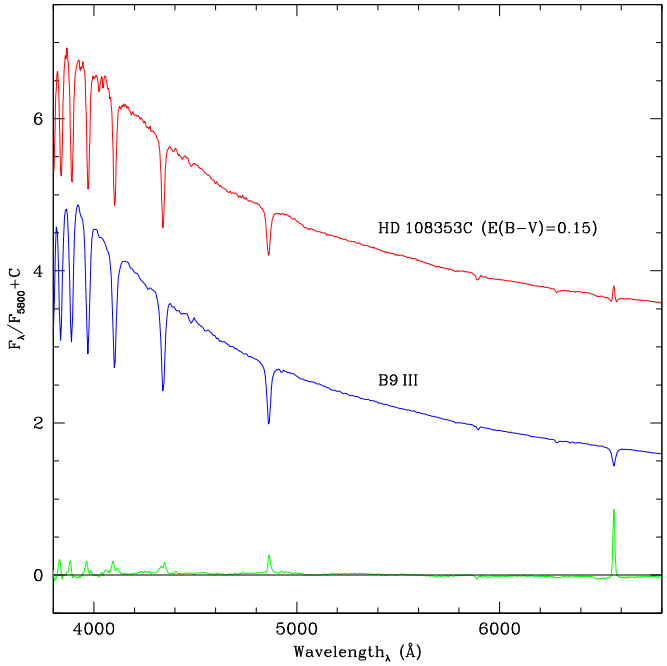

Fig. 7. Individual spectrum of one of the dominant stars of Harvard 5 (HD 108353C) corrected for reddening (*top*), the SC92 template spectrum which best matches it (*middle*) and the flux residual according to (F_{star} - $F_{template}$) / F_{star} (*bottom*). Units as in Fig. 2. (For interpretation of the references to colour in this figure legend, the reader is referred to the web version of this article.)

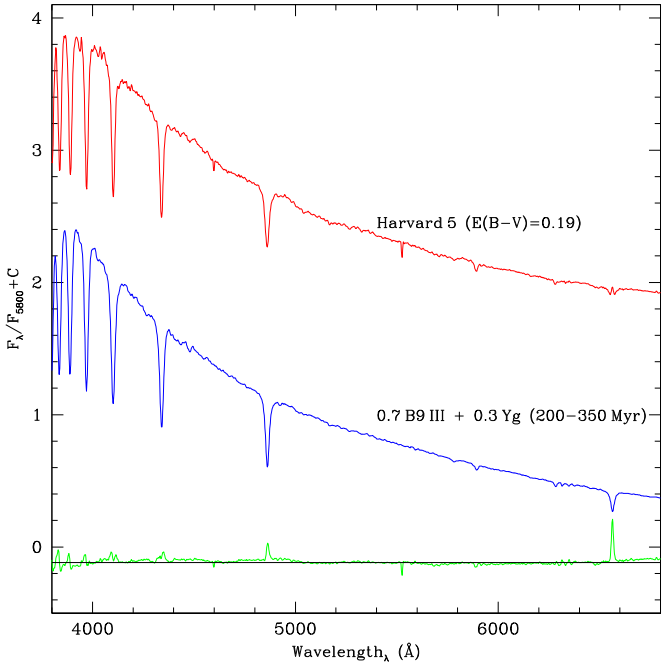

Fig. 8. Comparison between the reddening-corrected integrated spectum of Harvard 5, without the contribution of the comparatively bright blue star HD 108353A (*top*), with that of a combination of 70% of the spectrum of a B9 III template from SC92 and 30% of the Yg (200–350 Myr) template (*middle*). The corresponding flux residual according to ($F_{cluster}$ - $F_{template}$) / $F_{cluster}$ is shown at the bottom. Units as in Fig. 2. (For interpretation of the references to colour in this figure legend, the reader is referred to the web version of this article.)

corrected for $E(B-V) = 0.19$, matches very closely that of a combination of 70% of the spectrum of a B9 III template from SC92 and 30% of the P02's Yg (200–350 Myr) template (Fig. 8). The continuum distribution, the presence of the G-band (~4300 Å) and the intensity of the H and K Ca II lines in the observed spectrum favor the choice of the template Yg. Both the reddening value and the age of this template are consistent with the $E(B-V)$ color excess and with the earliest photometric spectral type (b3) estimated by MV73. The adopted reddening and age show also good agreement with the values reported by K13 and Clariá et al. (1989), respectively (Table 5).

As shown in Fig. 9, the individual spectrum of the comparatively bright MV73 star No. 8 (CPD-60°3999), corrected for $E(B-V) = 0.15$, is very similar to that of an A5/7 V template star from SC92. Consequently, this is very likely a cluster member. Besides, the individual spectra of MV73 stars 9 and 13, both corrected for $E(B-V) = 0.20$, clearly resemble the spectrum of a SC92's A1/3 V template (Fig. 10), so these two stars also turn out very probably to be cluster members. This is not the case, however, for MV73 No. 10, undoubtedly a foreground K5 V type star (Fig. 11). For the aforementioned reasons, the integrated spectrum of Harvard 5 includes the contributions of stars HD 108353B, HD 108353C, CPD-60°3999 and CPD-60°4002, but not the contribution of star MV73 10.

4.5. Hogg 14

Hogg 14 (IAU C1225-595), a sparse group of stars in Crux also known as MWSC 2037 (K12), was first recognised as a probable cluster by Hogg (1965a); 1965b). Like Harvard 5, Hogg 14 was classified as a Trumpler class II3p by AH03, i.e., a poor, detached cluster with bright and faint stars (Fig. 1). MV73 measured photoelectrically in the UBV system 11 stars located within a radius of ~3' centered at the star CD-59°4263 (Fig. 1). These stars seem to define an apparent sequence of a moderately young cluster reddened in average by $E(B-V) = 0.28$. In particular, the individual spectrum of the brightest star CD-59°4263 (MV73 No. 1), corrected for $E(B-V) = 0.22$, shows a reasonably good resemblance to the A3 III template from SC92 (Fig. 12), so this star seems to be an early A-type giant member of Hogg 14, which contributes to the integrated spectrum. On the other hand, the integrated spectrum of Hogg 14 corrected for $E(B-V) = 0.22$, matches closely that of a combination of 50% of the spectrum of an A3 III template from SC92 and 50% of the P02's Yg (200–350 Myr) template (Fig. 13). According to the Balmer-line method, Hogg 14 should be between 100 and 500 Myr old (Table 4), in good agreement with the template match. Then, we adopted $E(B-V) = 0.22 \pm 0.05$ and an age of 250± 100 Myr (Table 5) for Hogg 14, in accordance to the values reported by MV73 and K13. As for Ruprecht 158, radial velocity measurements of a few stars in the field of Hogg 14 could help to confirm or deny the physical reality of this cluster.

4.6. NGC 4463

This comparatively bright OC (IAU C1227-645) is probaby the most studied among those of the present cluster sample. Also known as Cr 260 (Collinder, 1931), Markarian 26 (Markarian, 1951), BH 135 (van den Bergh and Hagen, 1975) or MWSC 2042 (K12), this is a concentrated group o stars in the Musca constellation, classified as I3m by AH03 (Fig. 1). MV73 obtained UBV photoelectric photometry of 13 comparatively bright stars in the cluster field. They showed the reddening in front of NGC 4463 to be slightly variable, the mean value being $E(B-V) = 0.44$. In a more recent study, Delgado et al. (2011) estimated an age between 12 and 32 Myr and a mean color excess $E(B-V) = 0.39$, based on UBVRI photometry. These results show very good agreement with those derived by B11 from 2MASS data, while K13 estimated a somewhat older age (Table 5). On the other hand, using high-quality UBV-DDO data, Clariá et al. (1996) found the brightest star in the cluster field (MV73 No. 1 or CD-64°1943) to be an F-type

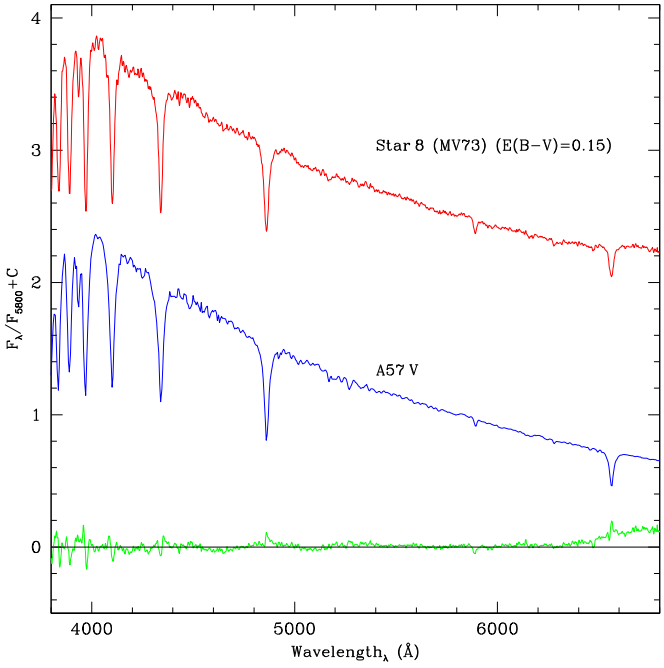

Fig. 9. Individual spectrum of star MV73 No. 8 (Fig. 1) of Harvard 5 corrected for $E(B-V) = 0.15$ (*top*), SC92 template spectrum which best matches it (*middle*) and flux residual according to (F_{star} - $F_{template}$) / F_{star} (*bottom*). Units as in Fig. 2.

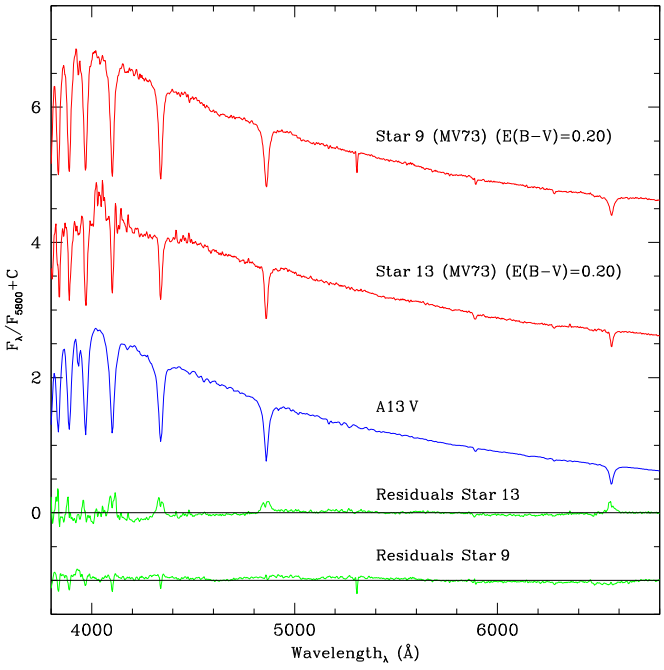

Fig. 10. From top to bottom : individual spectra of stars MV73 9 and 13 of Harvard 5 both corrected for $E(B-V) = 0.20$, SC92 template spectrum which best matches them and the corresponding flux residuals according to (F_{star} - $F_{template}$) / F_{star} (*bottom*). Units as in Fig. 2.

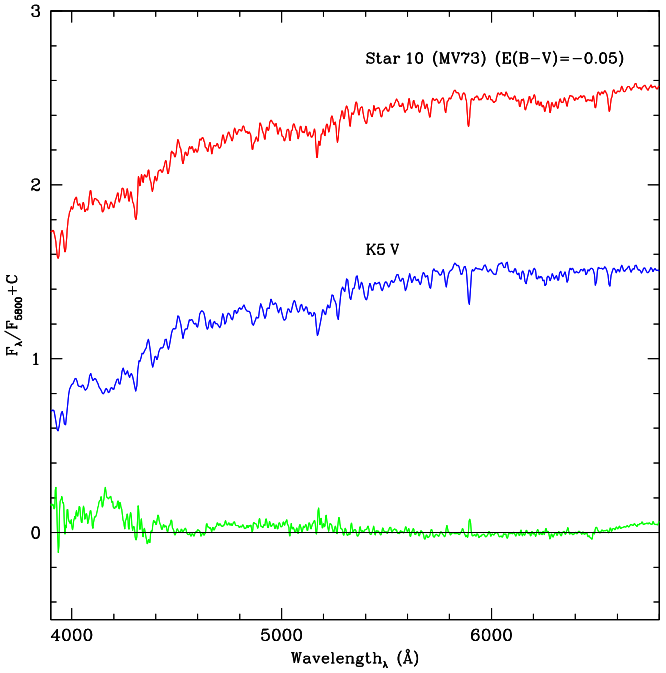

Fig. 11. Individual spectrum of the star MV73 No. 10 of Harvard 5 corrected for $E(B-V) = -0.05$ (*top*), SC92 template spectrum which best matches it (*middle*) and flux residual according to (F_{star} - $F_{template}$) / F_{star} (*bottom*). Units as in Fig. 2.

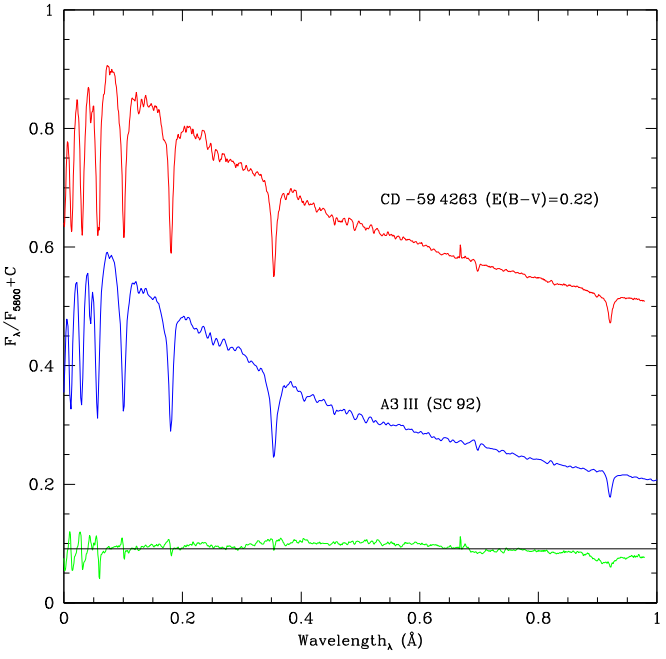

Fig. 12. Individual spectrum of the brightest star of Hogg 14 (CD-59°4263, MV73 No. 1) corrected for $E(B-V) = 0.22$ (*top*), SC92 template spectrum which best matches it (*middle*) and flux residual according to (F_{star} - $F_{template}$) / F_{star} (*bottom*). Units as in Fig. 2.

luminous star very probably non cluster member. Fig. 14 shows the cluster spectrum, corrected for $E(B-V) = 0.42$ and without the contribution of CD-64°1943, compared to the P02's Yb1 template of 5-10 Myr. Judging from the resultant residual flux, the similarity between these two spectra is evident. The weakness of the Balmer absorption lines in the cluster spectrum, however, suggests an age between 10 and 50 Myr. An alternative match is shown in the same figure, where we compare the spectrum of NGC 4463, corrected for $E(B-V) = 0.45$, with the older Ycd template of 30 Myr from Ahumada et al. (2007a). In the first case, there is a more evident similarity when the continuum distribution for $\lambda < 4000$ Å is considered. However, the opposite case results when the continuum distribution for $\lambda > 4000$ Å is compared. For NGC 4463 we adopted reddening and age values between those of these two templates, i.e., $E(B-V) = 0.43 \pm 0.03$ and 19 ± 10 Myr, which show very good agreement with most of the parameters reported in the literature (Table 5).

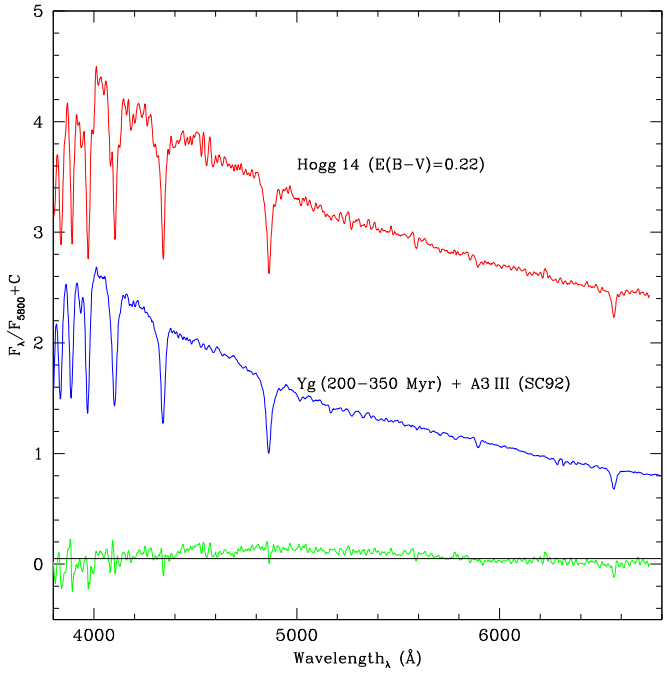

Fig. 13. Comparison between the reddening-corrected integrated spectum of Hogg 14 (*top*), with that of a combination of 50% of the spectrum of an A3 III template from SC92 and 50% of the P02's Yg (200–350 Myr) template (*middle*). The corresponding flux residual according to ($F_{cluster}$ - $F_{template}$) / $F_{cluster}$ are shown at the bottom. Units as in Fig. 2. (For interpretation of the references to colour in this figure legend, the reader is referred to the web version of this article.)

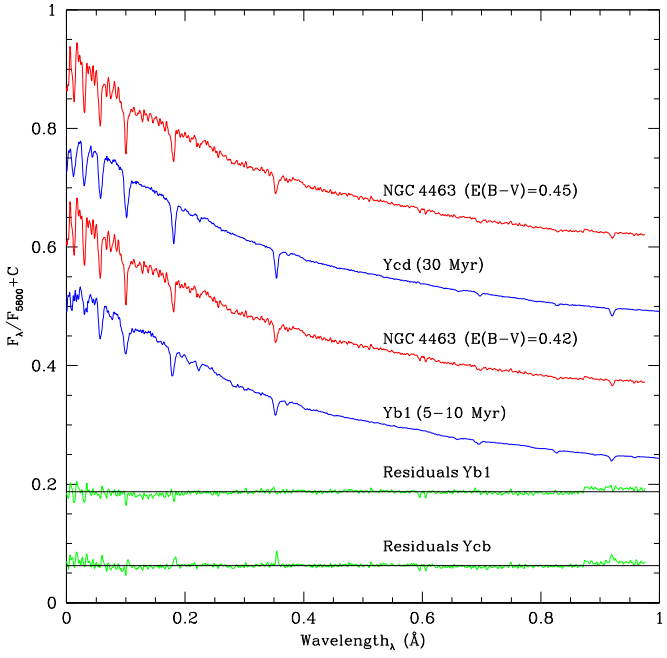

Fig. 14. Comparison between the reddening-corrected integrated spectrum of NGC 4463, without the contribution of CD-64°1943, and the Yb1 and Ycd templates spectra. The correspoding flux residuals according to ($F_{cluster}$ - $F_{template}$) / $F_{cluster}$ is shown at the bottom. Units as in Fig. 2.

4.7. ESO 065-SC07

This small group of stars in Musca, also designated as MWSC 2124 (K12), was first recognized as an OC by Lauberts (1982). ESO 065-SC07 barely stands out as a small handful of comparatively bright stars without central concentration (Fig. 1). AH03

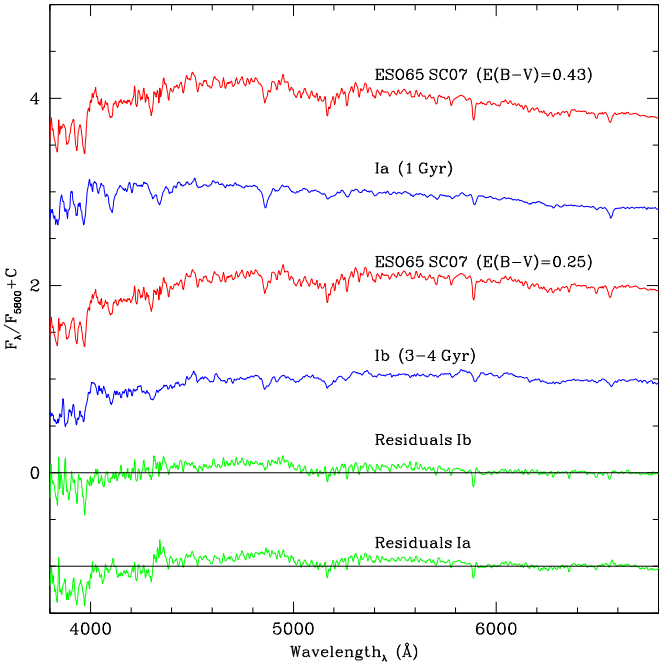

Fig. 15. From top to bottom: integrated spectrum of ESO 065-SC07 corrected for $E(B-V) = 0.43$, Ia template spectrum of 1 Gyr, cluster spectrum corrected for $E(B-V) = 0.25$, Yb template spectrum of (3-4 Gyr), and corresponding flux residuals between both comparisons. Units as in Fig. 2.

refer to it as belonging to Trumpler class III2. For ESO 065-SC07, K13 derived $E(B-V) = 0.29$ and an age of 2.5 Gyr, while B11 reported 0.48 and 1.23 Gyr, respectively. Fig. 15 shows comparisons of the reddening-corrected integrated cluster spectrum with both Ia (1 Gyr) and Ib (3-4 Gyr) templates from P02. In general terms, the integrated spectrum looks like both Ia and Ib templates, particularly in the presence and intensity of the spectral lines for wavelengths longer than 5000 Å. However, both spectral lines and molecular bands better resemble those of the oldest template Ib for shorter wavelengths. Note in the cluster integrated spectrum the presence of CN bands near 4200 Å, which are typical of old objects. Since the Balmer age is 1–5 Gyr (Table 4), we adopted for ESO 065-SC07 the average of the two considered template ages and reddenings, i.e., $E(B-V) = 0.34 \pm 0.05$ and 2.2 ± 1 Gyr (Table 5), in good agreement with the parameters reported by K13.

The reddening-corrected individual spectrum of the brightest star in the cluster field (TYC 9246-912-1, Fig. 1), compared with the K2 III template from SC92's library, is shown in Fig. 16. This comparison, together with the position of TYC 9246-912-1 in the CMDs of K13 and the acceptable coincidence between the color excess derived for ESO 065-SC07 and that of this star, support the conclusion that TYC 9246-912-1 is a red giant cluster member. The same occurs for the comparatively bright stars 23 and TYC 9250-1879-1, whose individual spectra, corrected by $E(B-V)$ of 0.30 and 0.20, respectively, resemble those of the K2 III template from SC92 (Fig. 17). Therefore, the contributions of stars TYC 9246-912, TYC 9250-1879-1 and 23 are included in the cluster integrated spectrum.

4.8. Pismis 23

Also known as BH 190 (van den Bergh and Hagen, 1975), Lynga 10 (Lyngå, 1965), ESO 226-SC05 (Lauberts, 1982) or MWSC 2399 (K12), this very small object was first recognized as an OC in Norma by Pišmiš (1959). Classified as III-2m by AH03 and located at about 25° from the Galactic center direction, Pismis

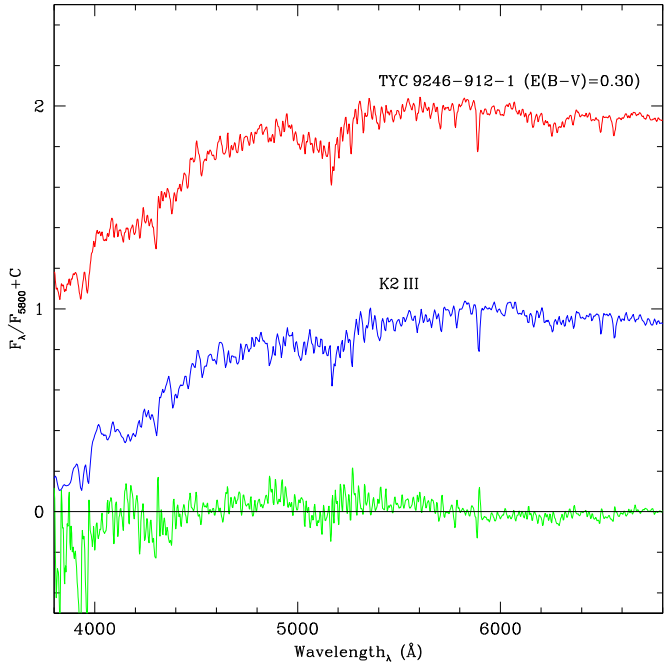

Fig. 16. Individual spectrum of the brightest star of ESO 065-SC07 (TYC 9246-912-1, Fig. 1) corrected for $E(B-V) = 0.30$ (*top*), SC92 template spectrum which best matches it (*middle*) and flux residual according to (F_{star} - $F_{template}$) / F_{star} (*bottom*). Units as in Fig. 2.

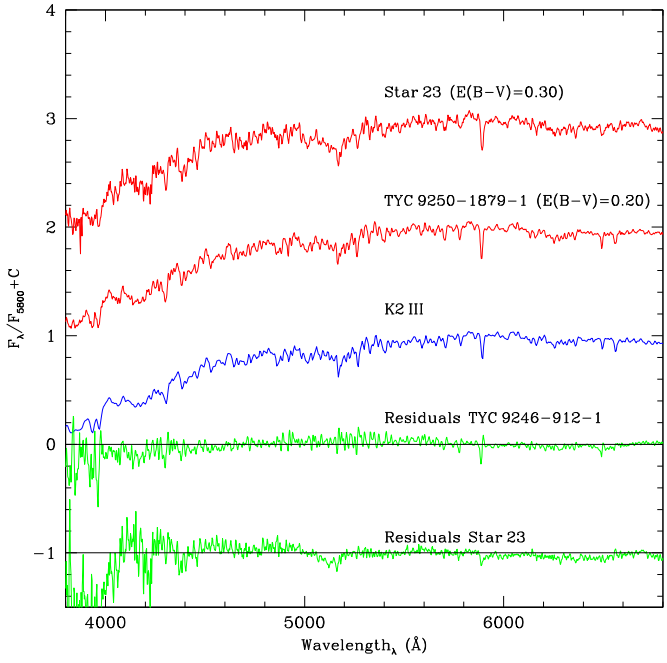

Fig. 17. From top to bottom: individual spectra of stars 23 and TYC 9250-1879-1 of ESO 065-SC07 (Fig. 1) corrected for $E(B-V) = 0.20$ and 0.30, respectively, SC92 template spectrum which best matches them and corresponding flux residuals according to (F_{star} - $F_{template}$) / F_{star}) (*bottom*). Units as in Fig. 2.

23 can easily be identified by its relatively dense population compared to that of the field stars (Fig. 1). The Balmer absorption lines indicate an age betwen 100 and 500 Myr (Table 4), while the cluster integrated spectrum, corrected for $E(B-V) = 1.05$, matches very closely that of the P02's Yg template of 200–350 Myr (Fig. 18). The spectrum of Pismis 23 presents Hα in emission, which is not expected at the age of the cluster. This emission arises from contamination of a neighbouring H II region at α = 16h 23m 49s, δ = −48º 54' 02", with diameter that can be easily seen with WISE Aladin. The adopted age for Pismis 23 shows good agreement with some of its previous age determinations (Table 5). Pismis 23 is the most reddened cluster in our sample, which can be explained by its association to gas and dust. Pismis 23's line of sight has important dust absorption and emitting gas. This can be explained by the projected neighbouring H II region's gas and dust. In this interpretation, the H II region would be in the foreground of the cluster.

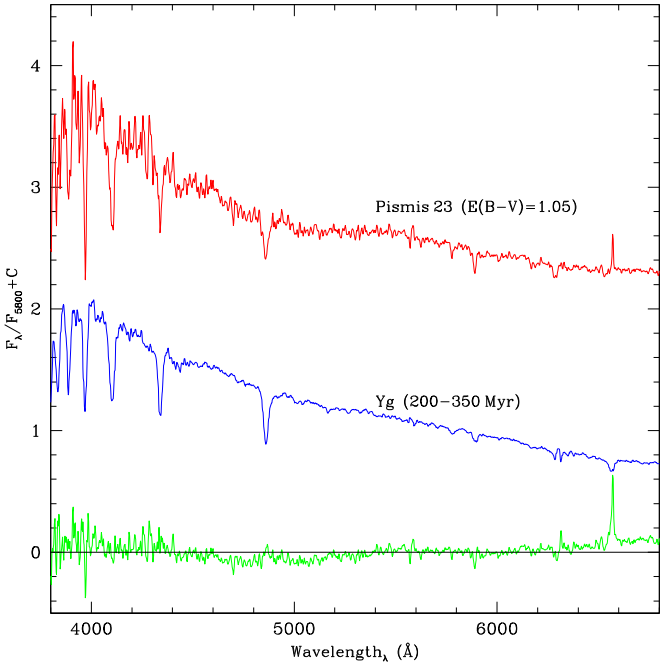

Fig. 18. Comparison between the reddening-corrected integrated spectrum of Pismis 23 (*top*) and the Yg template spectrum of (200–350 Myr) (*middle*). The corresponding flux residual according to ($F_{cluster}$ - $F_{template}$) / $F_{cluster}$ is shown at the bottom. Units as in Fig. 2.

4.9. Ruprecht 122

This small size cluster in Scorpius (IAU C1651-408), also referred to as BH 202 (van den Bergh and Hagen, 1975) or MWSC 2486 (K12), is projected on the South-West region of the extended complex called Trumpler 24 (Fig. 1), probably an stellar association with the IC 4628 nebulosity involved on its northern side (Heske and Wendker, 1984, AH03,K13,). Ruprecht 122 is located at about 15º from the Galactic center direction. Based on NIR photometric data, B11 derived for this cluster $E(B-V) = 0.87$ and log t = 8.05 (112 Myr), while K13 reported $E(B-V) = 0.42$ and log t = 7.6 (40 Myr). Despite its S/N ratio being rather low, the integrated spectrum of Ruprecht 122 shows typical features of a young cluster (Fig. 2), while the Balmer-line method yields an age between 10 and 50 Myr (Table 4). We find a good resemblance of the integrated spectrum to the P02's Yd template of 40 Myr, once the former was previously corrected for $E(B-V) = 0.45$ (Fig. 19). The continuum distribution, the Balmer jump and also the appearance and depth of the spectral lines are nearly identical in both spectra. Therefore, the parameters here derived for Ruprecht 122 show an excellent agreement with those reported by K13. In Fig. 20 we show that the individual spectrum of the comparatively bright star HD 322308, reddened by $E(B-V) = 0.10$, compares well with the K2 III template from SC92. Since HD 322308 falls clearly outside the cluster sequence (see CMDs from K13), we believe that this is

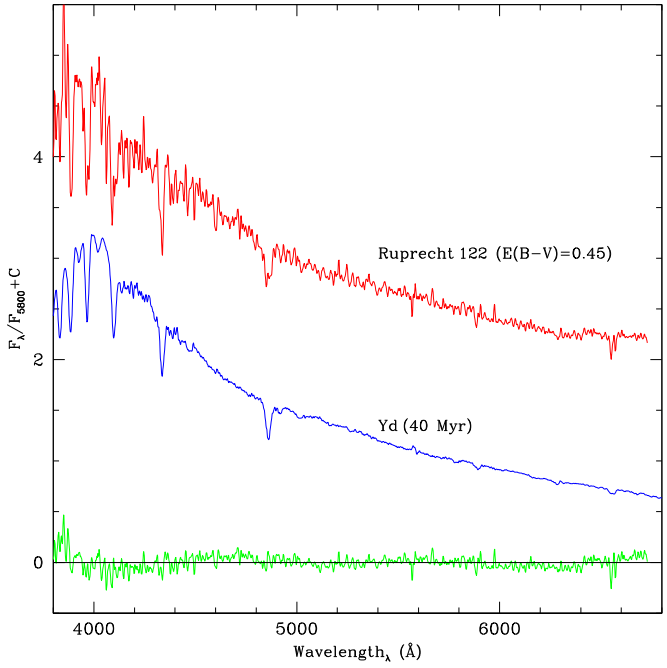

Fig. 19. Comparison between the reddening-corrected integrated spectrum of Ruprecht 122 (*top*) and the Yd template spectrum of 40 Myr (*middle*). The corresponding flux residual according to ($F_{cluster}$ - $F_{template}$) / $F_{cluster}$ is shown at the bottom. Units as in Fig. 2. (For interpretation of the references to colour in this figure legend, the reader is referred to the web version of this article.)

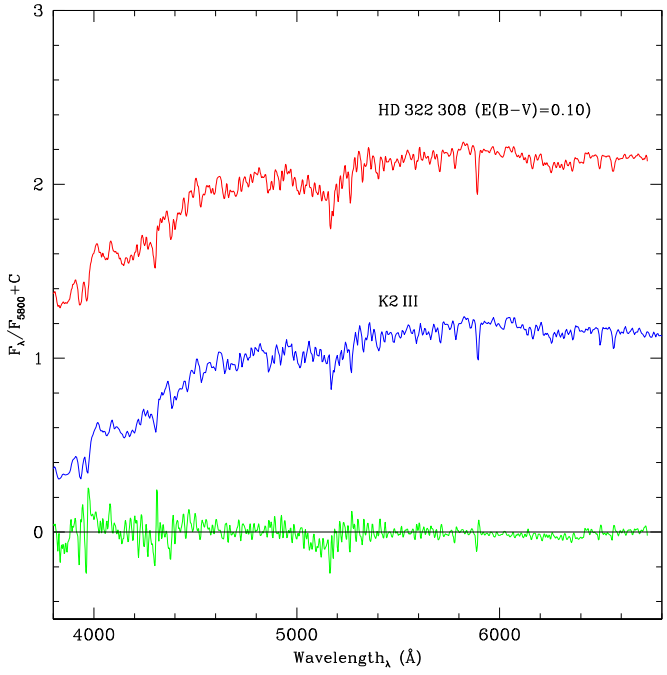

Fig. 20. Individual spectrum of the comparatively bright star HD 322308 in the field of Ruprecht 122 corrected for reddening (*top*), SC92 template spectrum which best matches it (*middle*) and flux residual according to (F_{star} - $F_{template}$) / F_{star} (*bottom*). Units as in Fig. 2.

a late-type foreground giant star so it was not included in the integrated spectrum.

5. Conclusions

As part of a systematic spectroscopic survey of small angular diameter Galactic OCs, we have increased the sample of studied

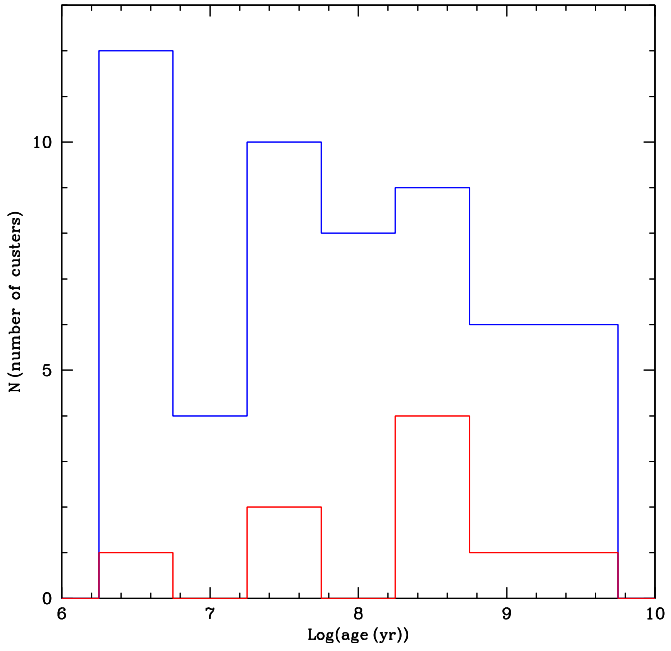

Fig. 21. Age distribution of the studied OCs. The blue line represents the sum of the previous and present cluster samples, while the red line stands only for the present sample.For interpretation of the references to colour in this figure legend, the reader is referred to the web version of this article.

southern Galactic OCs by means of integrated spectroscopy in the optical range. Using template spectra and equivalent widths of the Balmer lines, we determined ages and foreground reddening values for 9 small size OCs located in a 86^o sector centered at $l = 303^o$. Although all these clusters have basic parameters derived using NIR data from the 2MASS catalog, their integrated spectra provide independent information about their reddenings and ages. Individual spectra of some comparatively bright stars in the field of 5 out of the 9 studied OCs allowed us to evaluate their cluster membership status. Using 2MASS data is good and reliable for clusters which are well defined and clearly distinguishable from their surrounding regions, which may not always be the case. In fact, after a thorough analysis of the major large scale OC homogeneous parameter databases, Netopil et al. (2015) detected some trends and/or significant constant offsets. According to these authors, the databases can in some cases have 20% or more problematic objects, which might limit the usefulness of these databases. The present cluster sample complements that of 46 OCs we previously studied through integrated spectroscopy. Fig. 21 compares the age distribution of the sum of the previous and present cluster samples (blue line) with that of the here studied 9 OCs (red line). Despite the present efforts, the increase of the cluster spectroscopic base still requires clusters typically older than 500 Myr.

Excepting for Ruprecht 158 and BH 92, the results obtained in this study do agree, in general terms, with other findings reported in the literature. The best agreement to our results is found from those determinations based on optical data (e.g., UBV and/or DDO). The present spectroscopic results for Ruprecht 158 and BH 92, however, exhibit some differences with those reported by K13 and B11. Ruprecht 158 would seem to be a practically unreddened intermediate-age OC, somewhat younger than it was previously believed, while BH 92 appears to be somewhat younger than was reported by K13 but clearly older than estimated by B11. A more detailed study of these two clusters is then recommended.

The derived reddening values range from $E(B-V) \approx 0.0$ in Ruprecht 158 to $E(B-V) = 1.1$ in Pismis 23. We found that Cr 249, NGC 4463 and Ruprecht 122 are very young or young OCs (3-40

Myr). On the other hand, BH 92, Harvard 5, Hogg 14 and Pismis 23 are moderately young (200–400 Myr), while Ruprecht 158 and ESO 065-SC07 are intermediate-age objects (1–2.2 Gyr). The current cluster sample complements that of 46 OCs previously studied by our group, thus improving the age resolution around solar metallicity in the cluster spectral library for stellar population synthesis.

Acknowledgements

A.V. Ahumada, M.C. Parisi and D.B. Pavani are gratefully indebted to the CASLEO staff for their hospitality and support during the observing runs. We appreciate the valuable comments of the referee, which helped us to improve the manuscript. This research was partially supported by the Argentinian institutions Consejo Nacional de Investigaciones Científicas y Técnicas (CONICET), SECYT (Universidad Nacional de Córdoba) and Agencia Nacional de Promoción Científica y Tecnológica (ANPCyT). E. Bica acknowledges a grant from the Brazilian institution CNPq. This research has made use of NASA's Astrophysics Data System Bibliographic Services as well as of the SIMBAD database, operated at CDS, Strasbourg, France. We also made use of the VizieR catalogue access tool, CDS, Strasbourg, France. The original description of the VizieR service was published in A&AS 143, 23.

References

Ahumada, A.V., Benítez Llambay, A., Santos Jr., J.F.C., Clariá, J.J., Bica, E., Piatti, A.E., 2011. EFOSC2/NTT integrated spectroscopy of ten Magellanic Clouds' stellar clusters 40. 264–264

Ahumada, A.V., Clariá, J.J., Bica, E., 2007a. Integrated spectral properties of 22 small angular diameter galactic open clusters. A&A 473, 437–444. doi:10.1051/0004-6361:20077608.

Ahumada, A.V., Clariá, J.J., Bica, E., Dutra, C.M., Torres, M.C., 2001. Reddening and age for 13 southern Galactic open clusters determined from integrated spectra. A&A 377, 845–853. doi:10.1051/0004-6361:20011133.

Ahumada, A.V., Clariá, J.J., Bica, E., Pavani, D.B., Parisi, M.C., Palma, T., 2007b. Fundamental parameters of 6 southern galactic open clusters determined by means of integrated spectroscopy. Boletín de la Asociación Argentina de Astronomía, La Plata, Argentina 50, 81–84.

Ahumada, A.V., Clariá, J.J., Bica, E., Piatti, A.E., 2000. Integrated spectral properties of 7 galactic open clusters. A&AS 141, 79–88. doi:10.1051/aas:2000110.

Archinal, B.A., Hynes, S.J., 2003. Star clusters. Willman Bell, Inc. (AH03).

Barbá, R.H., Roman-Lopes, A., Nilo Castellón, J.L., Firpo, V., Minniti, D., Lucas, P., Emerson, J.P., Hempel, M., Soto, M., Saito, R.K., 2015. Hundreds of new cluster candidates in the VISTA Variables in the Vía Láctea survey DR1. A&A 581, A120. doi:10.1051/0004-6361/201424048.

Baume, G., Rodríguez, M.J., Corti, M.A., Carraro, G., Panei, J.A., 2014. A deep and wide-field view at the IC 2944/2948 complex in Centaurus. MNRAS 443, 411–422. doi:10.1093/mnras/stu1108.

Benítez-Llambay, A., Clariá, J.J., Piatti, A.E., 2012. Fast integrated spectra analyzer: a new computational tool for age and reddening determination of small angular diameter open clusters. PASP 124, 173–184. doi:10.1086/664570.

Bica, E., 1988. Population synthesis in galactic nuclei using a library of star clusters. A&A 195, 76–92.

Bica, E., Alloin, D., 1986a. A base of star clusters for stellar population synthesis. A&A 162, 21–31.

Bica, E., Alloin, D., 1986b. A grid of star cluster properties for stellar population synthesis. A&AS 66, 171–179.

Bica, E., Alloin, D., 1987. Near-infrared spectral properties of star clusters and galactic nuclei. A&A 186, 49–63.

Bica, E., Dutra, C.M., Soares, J., Barbuy, B., 2003. New infrared star clusters in the northern and equatorial milky way with 2MASS. A&A 404, 223–232. doi:10.1051/0004-6361:20030486.

Bonatto, C., Kerber, L.O., Bica, E., Santiago, B.X., 2006. Probing disk properties with open clusters. A&A 446, 121–135. doi:10.1051/0004-6361:20053573.

Borissova, J., Bonatto, C., Kurtev, R., Clarke, J.R.A., Peñaloza, F., Sale, S.E., Minniti, D., Alonso-García, J., Artigau, E., Barbá, R., Bica, E., Baume, G.L., Catelan, M., Chenè, A.N., Dias, B., Folkes, S.L., Froebrich, D., Geisler, D., de Grijs, R., Hanson, M.M., Hempel, M., Ivanov, V.D., Kumar, M.S.N., Lucas, P., Mauro, F., Moni Bidin, C., Rejkuba, M., Saito, R.K., Tamura, M., Toledo, I., 2011. New Galactic star clusters discovered in the VVV survey. A&A 532, A131. doi:10.1051/0004-6361/201116662.

Borissova, J., Chené, A.-N., Ramírez Alegría, S., Sharma, S., Clarke, J.R.A., Kurtev, R., Negueruela, I., Marco, A., Amigo, P., Minniti, D., Bica, E., Bonatto, C., Catelan, M., Fierro, C., Geisler, D., Gromadzki, M., Hempel, M., Hanson, M.M., Ivanov, V.D., Lucas, P., Majaess, D., Moni Bidin, C., Popescu, B., Saito, R.K., 2014. New galactic star clusters discovered in the VVV survey. Candidates projected on the inner disk and bulge. A&A 569, A24. doi:10.1051/0004-6361/201322483.

Bragaglia, A., Tosi, M., 2006. The Bologna open cluster chemical evolution project: midterm results from the photometric sample. AJ 131, 1544–1558. doi:10.1086/499537.

Bukowiecki, Ł., Maciejewski, G., Konorski, P., Strobel, A., 2011. Open clusters in 2MASS photometry. I. Structural and basic astrophysical parameters. Acta Astron. 61, 231–246. (B11). 1107.5119.

Cardelli, J.A., Clayton, G.C., Mathis, J.S., 1989. The relationship between infrared, optical, and ultraviolet extinction. ApJ 345, 245–256. doi:10.1086/167900.

Chen, L., Hou, J.L., Wang, J.J., 2003. On the Galactic disk metallicity distribution from open clusters. I. New catalogs and abundance gradient. AJ 125, 1397–1406. doi:10.1086/367911.

Chen, Y.-P., Trager, S.C., Peletier, R.F., Lançon, A., Vazdekis, A., Prugniel, P., Silva, D.R., Gonneau, A., 2014. The X-shooter Spectral Library (XSL). I. DR1: near-ultraviolet through optical spectra from the first year of the survey. A&A 565, A117. doi:10.1051/0004-6361/201322505.

Chené, A.-N., Borissova, J., Bonatto, C., Majaess, D.J., Baume, G., Clarke, J.R.A., Kurtev, R., Schnurr, O., Bouret, J.-C., Catelan, M., Emerson, J.P., Feinstein, C., Geisler, D., de Grijs, R., Hervé, A., Ivanov, V.D., Kumar, M.S.N., Lucas, P., Mahy, L., Martins, F., Mauro, F., Minniti, D., Moni Bidin, C., 2013. Massive open star clusters using the VVV survey. II. Discovery of six clusters with Wolf-Rayet stars. A&A 549, A98. doi:10.1051/0004-6361/201220107.

Cid Fernandes, R., Sodré, L., Schmitt, H.R., Leão, J.R.S., 2001. A probabilistic formulation for empirical population synthesis: sampling methods and tests. MNRAS 325, 60–76. doi:10.1046/j.1365-8711.2001.04366.x.

Clariá, J.J., Lapasset, E., Minniti, D., 1989. Photometric metal abundances of high-luminosity red stars in young and intermediate-age open clusters. A&AS 78, 363–374.

Clariá, J.J., Mermilliod, J.-C., Piatti, A.E., Parisi, M.C., 2006. Photometric and Coravel observations of red giant candidates in three open clusters: membership, binarity, reddening and metallicity. A&A 453, 91–99. doi:10.1051/0004-6361:20054716.

Clariá, J.J., Piatti, A.E., Mermilliod, J.-C., Palma, T., 2008. Photometric membership and metallicities of red giant candidates in selected open clusters. Astronomische Nachrichten 329, 609. doi:10.1002/asna.200710970.

Clariá, J.J., Piatti, A.E., Osborn, W., 1996. DDO metal abundances of high-luminosity late-type stars in Galactic open clusters. PASP 108, 672. doi:10.1086/133784.

Collinder, P., 1931. On structural properties of open Galactic clusters and their spatial distribution. Catalog of open Galactic clusters.. Ann. Observ. Lund 2, B1–B46.

Costa, E., Moitinho, A., Radiszc, M., Muñoz, R.R., Carraro, G., Vázquez, R.A., Servajean, E., 2015. Insights into the properties of the Local (Orion) spiral arm. NGC 2302: First results and description of the program. A&A 580, A4. doi:10.1051/0004-6361/201525784.

Delgado, A.J., Alfaro, E.J., Yun, J.L., 2011. Physical parameters of pre-main sequence stars in open clusters. A&A 531, A141. doi:10.1051/0004-6361/201116491.

Dias, B., Coelho, P., Barbuy, B., Kerber, L., Idiart, T., 2010. Age and metallicity of star clusters in the small Magellanic cloud from integrated spectroscopy. A&A 520, A85. doi:10.1051/0004-6361/200912894.

Dias, W.S., Alessi, B.S., Moitinho, A., Lépine, J.R.D., 2002. New catalogue of optically visible open clusters and candidates. A&A 389, 871–873. doi:10.1051/0004-6361:20020668.

Dutra, C.M., Bica, E., Soares, J., Barbuy, B., 2003. New infrared star clusters in the southern Milky Way with 2MASS. A&A 400, 533–539. doi:10.1051/0004-6361:20030005.

Friel, E.D., 1995. The old open clusters of the Milky Way. ARA&A 33, 381–414. doi:10.1146/annurev.aa.33.090195.002121.

Hasegawa, T., Sakamoto, T., Malasan, H.L., 2008. New photometric data of old open clusters II. A dataset for 36 clusters. PASJ 60, 1267–1284. doi:10.1093/pasj/60.6.1267.

Heske, A., Wendker, H.J., 1984. UBV photometry of TR 24 and its relation to Sco OB1. A&AS 57, 205–212.

Hogg, A.R., 1965a. Catalogue of open clusters south of −45° declination.. Memoires Mount Stromlo Observ. 17, 1–17.

Hogg, A.R., 1965b. New southern open clusters. PASP 77, 440. doi:10.1086/128254.

Jablonka, P., Bica, E., Bonatto, C., Bridges, T.J., Langlois, M., Carter, D., 1998. Metallicity distribution of bulge globular clusters in M 31. A&A 335, 867–875.

Kharchenko, N.V., Piskunov, A.E., Schilbach, E., Röser, S., Scholz, R.-D., 2012. Global survey of star clusters in the Milky Way. I. The pipeline and fundamental parameters in the second quadrant. A&A 543, A156. doi:10.1051/0004-6361/201118708. (K12).

Kharchenko, N.V., Piskunov, A.E., Schilbach, E., Röser, S., Scholz, R.-D., 2013. Global survey of star clusters in the Milky Way. II. The catalogue of basic parameters. A&A 558, A53. doi:10.1051/0004-6361/201322302. (K13).

Lauberts, A., 1982. ESO/Uppsala survey of the ESO(B) atlas.

López Fernández, R., Cid Fernandes, R., González Delgado, R.M., Vale Asari, N., Pérez, E., García-Benito, R., de Amorim, A.L., Lacerda, E.A.D., Cortijo-Ferrero, C., Sánchez, S.F., 2016. Simultaneous spectroscopic and photometric analysis of galaxies with STARLIGHT: CALIFA+GALEX. MNRAS 458, 184–199. doi:10.1093/mnras/stw260.

Lyngå, G., 1965. Studies of the Milky Way from Centaurus to Norma. IV. Galactic structure.. Meddelanden fran Lunds Astronomiska Observatorium Serie II 142, 3–6.

Markarian, B.E., 1951. On the classification of open (galactic) stellar clusters. II. Preliminary list of open O-type star clusters.. Soobshcheniya Byurakanskoj Observatorii Akademiya Nauk Armyanskoj SSR, Erevan 9, 1–40.

Minniti, D., Clariá, J.J., Gómez, M.N., 1989. The atmospheric extinction at the Complejo Astronomico EL Leoncito and the Bosque Alegre station. actaa 158, 9–18. doi:10.1007/BF00637437.

Minniti, J.H., Ahumada, A.V., Clariá, J.J., Benítez-Llambay, A., 2014. Reddening and age of six poorly studied star clusters of the large Magellanic cloud derived from integrated spectra. A&A 565, A49. doi:10.1051/0004-6361/201323314.

Moffat, A.F.J., Vogt, N., 1973. Southern open stars clusters. III. UBV-Hbeta photometry of 28 clusters between galactic longitudes 297d and 353d. A&AS 10, 135. (MV73).

Monteiro, H., Dias, W.S., Hickel, G.R., Caetano, T.C., 2017. The OPD photometric survey of open clusters II. robust determination of the fundamental parameters of 24 open clusters. NewA 51, 15–27. doi:10.1016/j.newast.2016.08.001.

Nesterov, V.V., Kuzmin, A.V., Ashimbaeva, N.T., Volchkov, A.A., Röser, S., Bastian, U., 1995. The Henry draper extension charts: a catalogue of accurate positions, proper motions, magnitudes and spectral types of 86933 stars. A&AS 110.

Netopil, M., Paunzen, E., Carraro, G., 2015. A comparative study on the reliability of open cluster parameters. A&A 582, A19. doi:10.1051/0004-6361/201526372.

Ortolani, S., Bica, E., Barbuy, B., Momany, Y., 2002. The very reddened open clusters Pismis 23 (Lyngå 10) and Stephenson 2. A&A 390, 931–935. doi:10.1051/0004-6361:20020716.

Palma, T., Ahumada, A.V., Clariá, J.J., Bica, E., 2008. Integrated spectral properties of four previously unstudied small angular size galactic open clusters. Astronomische Nachrichten 329, 392. doi:10.1002/asna.200710964.

Piatti, A.E., Bica, E., Clariá, J.J., Santos, J.F.C., Ahumada, A.V., 2002. Integrated spectral evolution of Galactic open clusters. MNRAS 335, 233–240. doi:10.1046/j.1365-8711.2002.05630.x. (P02).

Piatti, A.E., Clariá, J.J., 2002. Two highly reddened young open clusters located beyond the Sagittarius arm. A&A 388, 179–188. doi:10.1051/0004-6361:20020540.

Pierce, M., Bridges, T., Forbes, D.A., Proctor, R., Beasley, M.A., Gebhardt, K., Faifer, F.R., Forte, J.C., Zepf, S.E., Sharples, R., Hanes, D.A., 2006. Gemini/GMOS spectra of globular clusters in the Virgo giant elliptical NGC 4649. MNRAS 368, 325–334. doi:10.1111/j.1365-2966.2006.10097.x.

Piskunov, A.E., Kharchenko, N.V., Röser, S., Schilbach, E., Scholz, R.-D., 2006. Revisiting the population of Galactic open clusters. A&A 445, 545–565. doi:10.1051/0004-6361:20053764.

Pišmiš, P., 1959. New southern Star clusters. Boletin de los Observatorios Tonantzintla y Tacubaya 2, 37–38.

Portegies Zwart, S.F., McMillan, S.L.W., Gieles, M., 2010. Young massive star clusters. ARA&A 48, 431–493. doi:10.1146/annurev-astro-081309-130834.

Ramírez Alegría, S., Borissova, J., Chené, A.-N., Bonatto, C., Kurtev, R., Amigo, P., Kuhn, M., Gromadzki, M., Carballo-Bello, J.A., 2016. Massive open star clusters using the VVV survey. V. Young clusters with an OB stellar population. A&A 588, A40. doi:10.1051/0004-6361/201526618.

Ramírez Alegría, S., Borissova, J., Chené, A.N., O'Leary, E., Amigo, P., Minniti, D., Saito, R.K., Geisler, D., Kurtev, R., Hempel, M., Gromadzki, M., Clarke, J.R.A., Negueruela, I., Marco, A., Fierro, C., Bonatto, C., Catelan, M., 2014. Massive open star clusters using the VVV survey. III. A young massive cluster at the far edge of the Galactic bar. A&A 564, L9. doi:10.1051/0004-6361/201322619.

Roeser, S., Demleitner, M., Schilbach, E., 2010. The PPMXL catalog of positions and proper motions on the ICRS. Combining USNO-B1.0 and the Two Micron All Sky Survey (2MASS). AJ 139, 2440–2447. doi:10.1088/0004-6256/139/6/2440.

Santos Jr., J.F.C., Bica, E., 1993. Reddening and age for 11 Galactic open clusters from integrated spectra. MNRAS 260, 915–924. doi:10.1093/mnras/260.4.915.

Santos Jr., J.F.C., Bica, E., Dottori, H., 1990. Spectral synthesis aided by the H-R diagram - the open cluster M 11. PASP 102, 454–462. doi:10.1086/132654.

Santos Jr., J.F.C., Clariá, J.J., Ahumada, A.V., Bica, E., Piatti, A.E., Parisi, M.C., 2006. Spectral evolution of star clusters in the large Magellanic cloud. I. Blue concentrated clusters in the age range 40-300 Myr. A&A 448, 1023–1030. doi:10.1051/0004-6361:20054299.

Schiavon, R.P., Rose, J.A., Courteau, S., MacArthur, L.A., 2005. A library of integrated spectra of Galactic globular clusters. ApJS 160, 163–175. doi:10.1086/431148.

Seaton, M.J., 1979. Interstellar extinction in the UV. MNRAS 187, 73P–76P. doi:10.1093/mnras/187.1.73P.

Shapley, H., 1930. Star clusters. Harvard Observ. Monogr. 2.

Silva, D.R., Cornell, M.E., 1992. A new library of stellar optical spectra. ApJS 81, 865–881. doi:10.1086/191706. (SC92).

Skrutskie, M.F., Cutri, R.M., Stiening, R., Weinberg, M.D., Schneider, S., Carpenter, J.M., Beichman, C., Capps, R., Chester, T., Elias, J., Huchra, J., Liebert, J., Lonsdale, C., Monet, D.G., Price, S., Seitzer, P., Jarrett, T., Kirkpatrick, J.D., Gizis, J.E., Howard, E., Evans, T., Fowler, J., Fullmer, L., Hurt, R., Light, R., Kopan, E.L., Marsh, K.A., McCallon, H.L., Tam, R., Van Dyk, S., Wheelock, S., 2006. The two micron all sky survey (2MASS). AJ 131, 1163–1183. doi:10.1086/498708.

Stone, R.P.S., Baldwin, J.A., 1983. Southern spectrophotometric standards for large telescopes. MNRAS 204, 347–353. doi:10.1093/mnras/204.2.347.

Straižys, V., 1992. Multicolor stellar photometry. Pachart Publishing House.

Talavera, M.L., Ahumada, A.V., Santos Jr., J.F.C., Clariá, J.J., Bica, E., Parisi, M.C., Torres, M.C., 2010. Integrated spectroscopic study of 7 star clusters in the small Magellanic cloud. Astronomische Nachrichten 331, 323. doi:10.1002/asna.200911299.

Trancho, G., Bastian, N., Miller, B.W., Schweizer, F., 2007. Gemini spectroscopic survey of young star clusters in merging/Interacting Galaxies. II. NGC 3256 clusters. ApJ 664, 284–295. doi:10.1086/518886.

Trumpler, R.J., 1930. Preliminary results on the distances, dimensions and space distribution of open star clusters. Lick Observ. Bull. 14, 154–188. doi:10.5479/ADS/bib/1930LicOB.14.154T.

van den Bergh, S., Hagen, G.L., 1975. Uniform survey of clusters in the southern Milky Way.. AJ 80, 11–16. doi:10.1086/111707.

Vázquez, R.A., Moitinho, A., Carraro, G., Dias, W.S., 2010. Open clusters in the third Galactic quadrant III. Alleged binary clusters. A&A 511, A38. doi:10.1051/0004-6361/200811583.